Kinetic Folding Pathway of a Three-Disulfide Mutant of Bovine Pancreatic Ribonuclease A Missing the [40−95] Disulfide Bond†

Xiaobing Xu‡ and Harold A. Scheraga*

Baker Laboratory of Chemistry, Cornell University, Ithaca, New York 14853-1301

Received January 12, 1998; Revised Manuscript Received March 24, 1998

ABSTRACT: The oxidative refolding pathway of a three-disulfide mutant of bovine pancreatic ribonuclease A (RNase A) from the fully reduced unfolded form to the native state has been studied by using oxidized and reduced dithiothreitol as the redox reagents at pH 8.0 and 25 °C. This mutant was prepared by replacing Cys40 and Cys95 in RNase A with alanines while maintaining the other three native disulfide bonds to mimic one of the two major three-disulfide intermediates (des-[40−95]) observed in the regeneration of wild-type RNase A. The kinetics of refolding of this mutant were measured by quenching the regeneration reaction at various times with a rapid blocking reagent, 2-aminoethyl methanethiosulfonate (AEMTS), fractionating the disulfide intermediates by using cation-exchange HPLC, and analyzing the time course of each group of disulfide species. It was found that the disulfide intermediates formed during regeneration reach a steady-state distribution after a short period of preequilibration similar to that in the regeneration of wild-type RNase A. The experimental data acquired under different redox conditions were fit to a kinetic model with a steady-state treatment. The fitted results indicate that this mutant refolds through a rate-determining step which involves the oxidation of certain two-disulfide species to form a putative three-disulfide species which proceeds rapidly to the native protein. A rough estimation suggests that this pathway could constitute no more than 5% of the major pathway leading to the formation of des-[40−95] (the major three-disulfide intermediate formed) in the regeneration of wild-type RNase A. Several kinetic constants pertaining to the oxidation and reduction of various disulfide intermediates were compared with those obtained in the regeneration studies of wild-type RNase A to gain further understanding about the folding pathways of RNase A. Comparisons are also given for the oxidative refolding studies of several other three disulfide bond proteins, suggesting that the formation of a large number of disulfide-bonded intermediates during oxidative refolding is probably a common feature for most proteins.

Considerable effort has been made to elucidate the mechanisms for folding a polypeptide chain into a unique well-defined three-dimensional structure. Most experimental work has been concentrated on identifying the folding pathways that an unfolded protein takes to form the folded structure (*1*−*4*). A classical approach is to make use of the formation of disulfide bonds in proteins (*5*−*15*) because reduction of the disulfide bonds typically results in the unfolding of a protein. For proteins containing disulfide bonds, their folding processes are coupled with the formation of disulfide bonds to various degrees. In this approach, the folding process is typically initiated by mixing the fully reduced and denatured protein with a redox couple such as GSSG/GSH[1] or DTT^{ox}/DTT^{red}, and the subsequent folding process is monitored by various techniques. Hence, the disulfide folding pathways can usually be identified. This approach permits the study of the kinetics and structures of disulfide-folding intermediates in great detail. It provides information about the interatomic interactions that are important for promoting the formation of the native structure, complementing the understanding gained from investigations of the folding of the disulfide-intact proteins.

Much research has been carried out in our laboratory (*6*, *10*−*16*) and elsewhere (*17*) to investigate the folding of bovine pancreatic ribonuclease A (RNase A) (a protein containing 124 residues and 4 disulfide bonds) by using the

† This work was supported by the National Institute of General Medical Sciences of the National Institutes of Health (Grant GM-24893). Support was also received from the National Foundation for Cancer Research. A brief report of these results was presented at the Protein Society meeting in San Jose, CA, August 1996 [Xu, X., and Scheraga, H. A. (1996) Regeneration of a three-disulfide mutant of ribonuclease A *Protein Sci. 5 (Suppl. 1)*, 139-M].

* Author to whom correspondence should be addressed.

‡ X.X. was a Leukemia Society of America Special Fellow, 1995−1997.

[1] Abbreviations: RNase A, bovine pancreatic ribonuclease A; BPTI, bovine pancreatic trypsin inhibitor; des-[40−95], a three-disulfide intermediate of ribonuclease A containing three native disulfide bonds, but lacking the disulfide bond between Cys40 and Cys95; des-[40−95]A, a mutant analog of des-[40−95] obtained by substituting alanines for Cys40 and Cys95 using site-directed mutagenesis; rHV1, recombinant hirudin variant 1; 1S, one-disulfide intermediates; 2S, two-disulfide intermediates; 3S, three-disulfide intermediates; 4S, four-disulfide intermediates; AEMTS, 2-aminoethyl methanethiosulfonate [$(NH_2)C_2H_4SSO_2CH_3$]; NTB, 2-nitro-5-thiobenzoate; MS, mass spectrometry; MALDI, matrix-assisted laser desorption ionization; ES, electron spray; HPLC, high-performance liquid chromatography; DTT^{red}, reduced dithiothreitol; DTT^{ox}, oxidized dithiothreitol; GSSG, oxidized glutathione; GSH, reduced glutathione; EDTA, ethylenediaminetetraacetic acid; GdnSCN, guanidine thiocyanate; HEPES, 4-(2-hydroxyethyl)-1-piperazineethanesulfonic acid; Tris, tris(hydroxymethyl)-aminomethane.

S0006-2960(98)00086-5 CCC: $15.00
Published on Web 04/22/1998

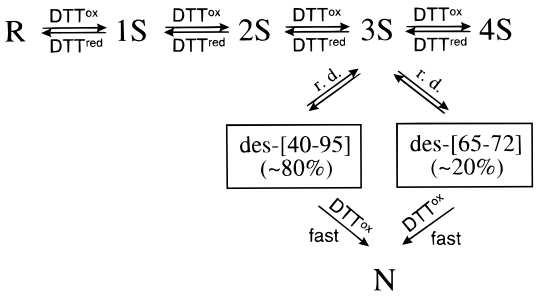

FIGURE 1: Regeneration pathways of RNase A using DTT^{ox} / DTT^{red} as redox reagents at 25 °C and pH 8.0, summarized from Rothwarf et al. (*15*). R and N represent the fully reduced and native proteins, respectively. 1S, 2S, 3S, and 4S represent one-, two-, three-, and four-disulfide-bonded intermediates, respectively, formed during regeneration; r.d. represents the rate-determining step; des-[40−95] and des-[65−72] represent two three-disulfide intermediates formed in a rate-determining step, each of them containing three native disulfide bonds, but missing the one disulfide bond denoted in brackets.

disulfide bond formation approach. The study of RNase A involves determining the kinetic pathways of folding, characterizing the disulfide folding intermediates, and determining the energetics and structural transitions occurring during folding. However, being a four-disulfide-bonded protein, the study of RNase A by disulfide bond formation is much more complicated than the study of proteins containing three or less disulfide bonds, because the number of disulfide intermediates grows considerably (*18*) as the number of disulfide bonds in a protein increases; e.g., there are 74 such species in a three-disulfide protein and 762 in a four-disulfide protein (excluding the native and reduced species). Therefore, identification of intermediates constituted the major barrier to solving the folding problem in RNase A in earlier years (*19*, *20*).

In recent years, significant progress has been made in studying the folding pathways of RNase A with the following modifications of several experimental techniques (*10*−*15*, *21*): (1) The regeneration pathway is studied using DTT^{ox}/ DTT^{red} (instead of GSSG/GSH) as the redox reagent; this virtually eliminates the formation of mixed disulfide bonds, greatly reducing the number of disulfide-bonded species involved in the regeneration process and simplifying the isolation and identification of disulfide-bonded intermediates. (2) A more effective blocking reagent, 2-aminoethyl methanethiosulfonate (AEMTS), is used instead of a conventional blocking reagent such as iodoacetic acid or iodoacetamide, permitting much faster quenching of free thiols, reducing the possibility of disulfide reshuffling during blocking. (3) The extra positive charge carried by the blocking reagent AEMTS enables the folding intermediates to be separated by ion-exchange chromatography according to the number of blocked cysteines. It also permits the isolation of intermediates for further characterization.

With the above modifications in techniques, the regeneration pathways of wild-type RNase A through disulfide bond formation have been well characterized (*10*−*15*) and are summarized in Figure 1. Upon refolding from the fully denatured and reduced ribonuclease A, groups of one-, two-, three-, and four-disulfide-bonded intermediates form sequentially. After an initial period, the concentrations of the disulfide-bonded intermediates and the reduced species reach a steady-state distribution. Fitting of the experimental data to kinetic models suggests that the rate-determining steps for the regeneration of wild-type RNase A are the rearrangements of some three-disulfide intermediates to form two three-disulfide species, des-[40−95] and des-[65−72], missing disulfide bond 40−95 or 65−72, respectively, both of which then proceed rapidly to form the native protein. The three-dimensional structures of these two three-disulfide intermediates were characterized in the form of cysteine-blocked intermediates (*22*) and of mutant analogs with alanine or serine substitutions for cysteines obtained by mutagenesis (*23*, *24*). Their structures were determined by multidimensional heteronuclear NMR spectroscopy, and were found to be similar to that of the native protein, but much more dynamic and susceptible to increased rates of hydrogen/deuterium exchange.

The three-disulfide intermediate des-[40−95] is particularly interesting, because it is responsible for the formation of more than 80% of the native protein during regeneration. A study of the distribution of one-disulfide intermediates formed during the regeneration of wild-type RNase A showed that the one-disulfide intermediate containing the native disulfide bond between Cys65 and Cys72 is particularly important, comprising 40% of the total one-disulfide population out of the 28 possible intermediates (*25*). The results suggest that the majority of the population may regenerate through formation of intermediates containing the disulfide bond between Cys65 and Cys72. It seems that formation of des-[40−95] represents a major pathway in the refolding of RNase A with possible preservation of disulfide bond [65−72] at various stages of regeneration. Therefore, a study of the oxidative regeneration of des-[40−95] is necessary to provide details of the regeneration of RNase A and to gain further understanding about its folding pathways.

However, it is not possible to study the regeneration of this three-disulfide intermediate directly as in the study of wild-type RNase A because the free thiols at Cys40 and Cys95 would interfere with the regeneration process. Therefore, we have prepared a three-disulfide mutant in which Cys40 and Cys95 were replaced by alanines to mimic this disulfide intermediate. This species is denoted as des-[40−95]A. Study of the refolding of des-[40−95]A can serve several purposes: (1) It can help in understanding the pathways for the formation of the true three-disulfide intermediate des-[40−95] during the regeneration of RNase A. Since pathways through disulfide rearrangements for the formation of des-[40−95] are blocked in this mutant analog, the study of this mutant can provide information about alternative pathways for the regeneration of RNase A. (2) It can help in studying early folding events in wild-type RNase A. Since there are only three disulfide bonds in the mutant protein, the identification of one- and two-disulfide intermediates will be greatly simplified. (3) By comparing the folding kinetics of the mutant with those of wild-type RNase A, the importance of disulfide bond formation involving Cys40 and Cys95 can be evaluated, which may provide information about conformational folding in regions involving Cys40 and Cys95. (4) Since this mutant contains three disulfide bonds, its folding kinetics can be compared directly with other three-disulfide-containing proteins studied so far, such as, BPTI, hirudin, and other proteins. In our laboratory, the oxidative regeneration of another three-disulfide mutant, des-[65−72]A (and des-[65−72]S), mim-

icking the other major three-disulfide intermediate des-[65−72], has also been studied (*26*). Such a comparison should provide useful information for understanding the differences in the folding kinetics in these proteins as well as information about the folding of wild-type RNase A.

In the present work, the regeneration of the folded mutant des-[40−95]A has been carried out by using DTT^{ox}/DTT^{red} as the redox reagents at 25 °C and pH 8.0. The kinetics of formation of various disulfide-bonded intermediates along the regeneration pathway are determined by quenching the reaction at various refolding times and isolating the disulfide-bonded species by cation-exchange HPLC. A refolding pathway of this mutant is proposed by fitting the kinetic data to a model which accounts for the data. The results are compared directly with those obtained from the regeneration studies of wild-type RNase A, thereby providing insights into the folding processes in both the mutant and wild-type RNase A. The results are also compared with oxidative folding studies of several other three-disulfide-containing proteins to gain further understanding about the nature of the interactions that influence protein folding through formation of disulfide bonds.

MATERIALS AND METHODS

Materials. The plasmid for the expression of mutant RNase A was constructed by inserting the RNase A gene between the *Msc*I and *Hin*dIII restriction sites in pET22b-(+) (Novagen) (*27*). The substitution of cysteines 40 and 95 was achieved by using site-directed mutagenesis using the T7-gen in vitro mutagenesis kit (United States Biochemical). The expression, purification, and refolding of the mutant des-[40−95]A have been described in detail elsewhere (*24*).

After refolding, the mutant protein was further purified on a preparative Hydropore-5-SCX column (21.4 × 100 mm) from Rainin, using a buffer of 25 mM HEPES, 1 mM EDTA, pH 7.0, and a linear gradient from 50 mM NaCl to 150 mM NaCl in 40 min. The protein appeared as the largest peak on the chromatogram. The purity of the purified protein was checked by reinjecting the purified protein on an analytical Hydropore-5-SCX column (4.6 × 150 mm) from Rainin. The purified protein was then concentrated, desalted, lyophilized, and stored in a desiccator in the cold room. The final yield of protein was 40−50 mg/L of culture.

The correctness of mutagenesis was confirmed using several methods: DNA sequencing, amino acid analysis of protein, and peptide-mapping of the expressed protein. The disulfide pairing in the folded protein was determined by peptide mapping with trypsin and chymotrypsin digestion, and was found to have the three native disulfide bonds 26−84, 58−110, and 65−72 as in wild-type RNase A.

DTT^{ox} (Sigma Chemical Co.) was purified by the method of Creighton (*5*). AEMTS was synthesized as described by Bruice and Kenyon (*28*). All other reagents were of the highest grade commercially available and were used without further purification.

Reduction and Regeneration of Des-[40−95]A. Approximately 10 mg of des-[40−95]A was reduced with 50 mM DTT^{red} in approximately 5 mL of buffer containing 0.1 M Tris, 3 mM EDTA, and 4 M GdnSCN at pH 8.0 for 2−3 h. The reduced protein was then desalted with 100 mM acetic acid (to remove DTT^{red} and salts such as Tris, EDTA, and GdnSCN) under constant argon sparging and lyophilized. The protein was then redissolved to a concentration of 8−9 mg/mL in 100 mM acetic acid and stored in a −70 °C freezer for future use. The concentration of protein was determined by an Ellman assay (*29*), using an extinction coefficient of 13 900 at 412 nm for NTB (*30, 31*). A check was made for possible degradation (due to deamidation) or oxidation of protein by blocking an aliquot of the reduced protein with AEMTS, and analyzing it on the cation-exchange HPLC. On the HPLC chromatogram, deamidated and oxidized proteins elute at different positions from the fully reduced and blocked protein. It was found that the reduced protein stored in 100 mM acetic acid at −70 °C can be kept intact for at least 6 months without deamidation or oxidation.

The procedure for regeneration was similar to the one described by Rothwarf and Scheraga (*10*). The regeneration process was initiated by adding an appropriate amount of the reduced protein (typically less than 200 μL of the concentrated solution) directly to 8 mL of predegassed refolding buffer containing 0.1 M Tris, 3 mM EDTA, and various concentrations of DTT^{ox} at pH 8.0. The solution was kept stirred under an atmosphere of argon and immersed in a water bath at 25 °C. The protein concentration was varied from 8.0 to 32 μM, and the initial concentration of DTT^{ox} was varied between 40 and 200 mM to achieve appreciable regeneration rates. No DTT^{red} was added initially, since the presence of a small amount of DTT^{red} may result in too slow a regeneration rate to be measured practically. DTT^{red} was generated during the regeneration process. The concentration of DTT^{red} increased rapidly at early regeneration times and reached a pre-equilibrium steady-state during regeneration, and was determined by the concentrations of both DTT^{ox} and protein used under each regeneration condition. More than 10 different combinations of protein and DTT^{ox} concentrations were used to carry out the regeneration experiments.

After initiation of the regeneration process, aliquots were taken at various refolding times and quenched with the rapid-blocking reagent AEMTS (approximately 20−50 times excess in concentration). The blocked aliquots were adjusted to pH 5.0 using concentrated acetic acid solution and frozen at −20 °C for further analysis. In a typical regeneration experiment, 12−14 aliquots were taken over a period of 7.5 h. Although longer regeneration times were used for further regeneration, only data obtained within the first 7.5 h were used in analysis, since adverse effects such as deamidation may occur at later times to complicate the analysis of the regeneration process (*10*). The exclusion of oxygen from the regeneration system was checked by measuring the total thiol concentrations before and after regeneration using Ellman's assay (*29*). The changes of thiol concentration were found to be less than 2% during the period of regeneration.

Regeneration was also initiated by the method of Rothwarf and Scheraga (*10*) by directly desalting the reduced protein into a 0.1 M Tris and 3 mM EDTA refolding buffer at pH 8.0, and then adding DTT^{ox} to the desired concentrations. Little difference was observed for the regeneration kinetics from those obtained using the first method. However, the first method provided easier handling of the experimental procedures as well as better control of protein concentration.

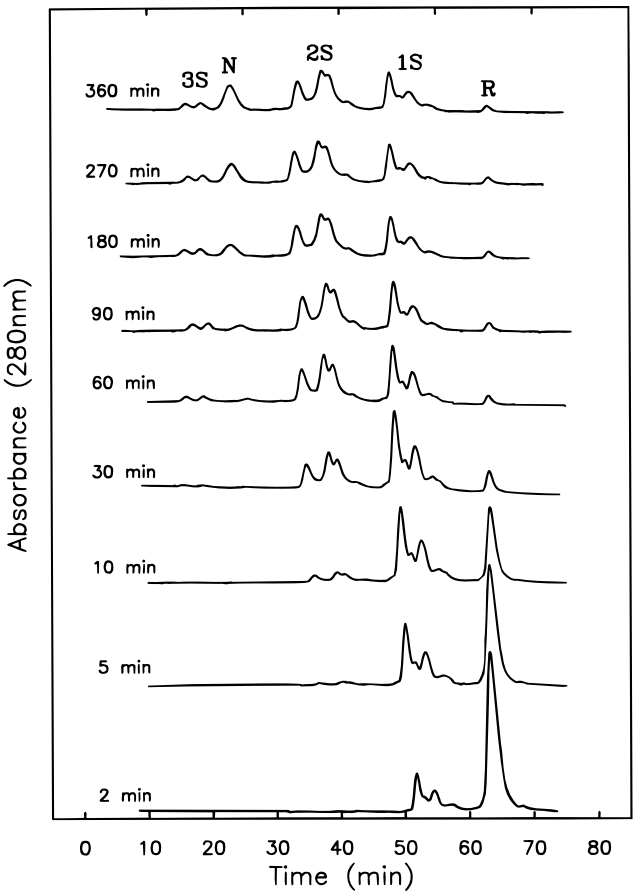

FIGURE 2: Series of chromatograms showing the appearance of various intermediates at the regeneration time indicated on each plot. The starting regeneration conditions were pH 8.0, 25 °C, 15 μM des-[40−95]A, 150mM DTT^{ox}, and 0 mM DTT^{red}.

Therefore, most experiments were carried out by the first method.

Analysis of Regeneration Process. The aliquots obtained during regeneration were analyzed by cation-exchange chromatography running on an HPLC system SP8800 from Spectra Physics. A ternary gradient system was used. Buffer A contained 25 mM HEPES and 1 mM EDTA at pH 7.0. Buffer B contained buffer A with 1 M NaCl. Buffer C contained 50 mM NaOAc at pH 5.0. In a typical analysis, buffer C was run first for 20 min to remove the salts, and then an NaCl gradient from 5% to 20% B in 75 min was run to resolve different disulfide-bonded intermediates. A Hydropore column (Hydropore-5-SCX, 4.6 × 50 mm) from Rainin was used for analysis. The use of such a column was necessary to ensure complete resolution of the native mutant from the disulfide-bonded intermediates. Proteins were detected using an ISCO UA-5 absorbance detector with a type 9 optical unit and a 280 nm filter.

Figure 2 shows the HPLC chromatograms of aliquots taken at various regeneration times using 15 μM protein and 150 mM DTT^{ox}. Assignments for species observed on the chromatogram are labeled on the top and were made based on the following arguments: (1) Since the blocking group that we used adds an additional single positive charge to each blocked cysteine, there are +6 extra charges for the fully reduced and blocked protein, +4 for the one-disulfide intermediates, and +2 for the two-disulfide intermediates. Therefore, it is expected that the fully reduced and blocked protein will elute at a later time on the cation-exchange chromatogram compared to other disulfide-bonded species. The three-disulfide species (with no additional positive charges) will elute first, followed by the two-disulfide species, and then the one-disulfide species. (2) The sequence of appearance of various disulfide-bonded species in the regeneration process also suggests their identities. It is conceivable that, upon oxidative formation of disulfide bonds from the fully reduced species, the one-disulfide species will form first, then the two-disulfide, and finally the three-disulfide species. (3) The identities of each group of intermediates were confirmed by both MALDI and ES mass spectroscopy. The mass difference between neighboring groups of intermediates was 152 daltons (the mass of two blocking groups). On MALDI-MS, a broad peak (due to dissociation of blocking groups) with its center at the expected mass was observed for each group of intermediates. On ES-MS, a single mass at the expected molecular weight was also observed for each group of intermediates.

The assignment for the regenerated native mutant was based on its retention time on the cation-exchange column. This species eluted at the same retention time as the intact mutant protein on the HPLC chromatogram, and exhibited a similar characteristic broad peak profile as well. The identity of this species was also confirmed by isolating it and carrying out peptide-mapping procedures. Almost identical peptide maps were obtained for this species as well as for the intact (un-reduced) des-[40−95]A mutant. In addition, the retention time of this native mutant provided further evidence for the assignment of this species. This three-disulfide species eluted between the two- and three-disulfide groups, contrary to the conventional expectation that it should elute prior to all the other three-disulfide intermediates. The true three-disulfide intermediate des-[40−95] formed during regeneration of RNase A also elutes after the three-disulfide intermediate group (*14*, *32*), indicating that the mutant analog mimics the charge property of the true three-disulfide intermediate. However, the reason why this three-disulfide species elutes at an abnormal retention time is not well understood yet.

Kinetic Analysis of Regeneration Process. The experimental data were interpreted by using an approach first developed by Konishi et al. (*33*), and further exploited by Rothwarf and Scheraga (*11*). The details of the treatment have been presented for regeneration of both wild-type RNase A (*11*) and a three-disulfide protein, recombinant hirudin variant 1 (rHV1) (*34*). In this approach, the reduced protein and the ensembles of 1S, 2S, and 3S intermediates are viewed as existing in a preequilibrium or steady-state condition. The ensembles of 1S, 2S, and 3S species are considered to be single kinetic species. This view is justified because the distribution of species within each ensemble does not vary significantly with regeneration times or redox conditions (see Results). The folding pathway is defined by the type of intermediate (1S, 2S, or 3S) and the type of disulfide exchange reaction (oxidation, reduction, or rearrangement) involved in the rate-determining step. For a three-disulfide protein like des-[40−95]A, there are 10 possible rate-determining steps. These are described in detail in the paper by Thannhauser et al. (*34*). The rate of appearance of the native protein (*N*) is given by the equation:

$$dN/dt = \sum_{i=1}^{3} k_i f_i (1 - N)[DTT^{ox}] + \sum_{i=1}^{4} k_i f_i (1 - N)[DTT^{red}] + \sum_{i=1}^{4} k_i f_i (1 - N) \quad (1)$$

Here, the quantity k_i is the apparent rate constant for the *i*th pathway and f_i is the fractional concentration of the *i*th grouping of intermediates in the regeneration reaction mixture. The experimentally determined concentrations of the species involved in the steady-state preequilibrium and the native protein as a function of time and redox condition were fit by 10 different refolding models (*34*). The mathematical treatment used for data fitting was exactly the same as described in the paper by Rothwarf and Scheraga (*11*). Each of the possible rate-determining steps was investigated. The single folding pathway that best fits all the experimental data from the regeneration at different redox conditions was chosen as the preferred pathway for regeneration. From the fitting, the rate constant for the regeneration of native protein as well as the rate constants for formation and reduction of disulfide bonds at different stages of regeneration could also be determined.

RESULTS

Steady-State Distribution of Disulfide Intermediates. For each regeneration condition, the intermediates formed along the regeneration pathway were fractionated using cation-exchange HPLC by analyzing aliquots quenched at various regeneration times. A series of chromatograms at various refolding times is shown in Figure 2 under the regeneration condition of 15 μM protein, 150 mM DTT^{ox}, 25 °C, and pH 8.0. The assignments for the peaks are labeled on the top curve. It must be kept in mind that each broad peak of the chromatogram represents an ensemble of disulfide-bonded species with the same number of disulfide bonds but with different disulfide pairings. For example, 1S represents a collection of one-disulfide intermediates that may possibly contain as many as 15 species with different disulfide pairings. It is seen from Figure 2 that the concentrations of the different species (except for the native peak) change rapidly at early regeneration times, but the populations of these species level off after a regeneration time of 60−90 min. The concentration of the native protein increases steadily with time. This behavior is seen more clearly from Figure 3 which plots the population changes of various disulfide species as a function of regeneration time under different regeneration conditions. The population change of different disulfide groupings for the regeneration condition of Figure 2 (15 μM protein, 150 mM DTT^{ox}, 25 °C, and pH 8.0) is plotted in panel b with various symbols. (The details of Figure 3 will be discussed in the text below.) It is clearly seen that, although the concentrations of the different disulfide intermediates decline slowly with regeneration time after 60−90 min, the fraction of each disulfide grouping relative to the total population of disulfide intermediates remains invariant with time. Therefore, we conclude that the populations of the disulfide-bonded intermediates reach a preequilibrium steady-state condition during the regeneration.

It is also important to note that the peak profiles on the HPLC chromatograms of Figure 2 for the different disulfide intermediates 1S, 2S, and 3S are invariant with regeneration time, even though their intensities are much smaller at early times. Although small shifts in retention times were observed for different disulfide species, especially at early times, this probably resulted from concentration differences for these species (which is a common chromatographic

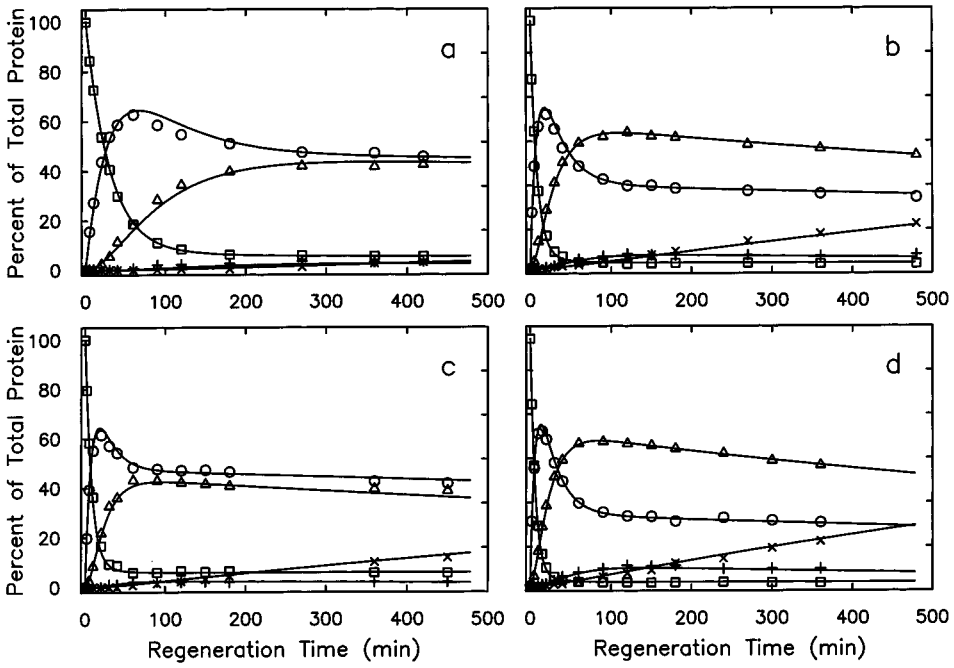

FIGURE 3: Concentration of various disulfide species (including the reduced and native proteins) as a function of regeneration time for des-[40−95]A at pH 8.0 and 25 °C. The symbols represent the experimental data: (□) reduced protein; (○) one-disulfides; (△) two-disulfides; (+) three-disulfides; and (×) native protein. The solid curves are theoretical fits based on the kinetic model discussed in the text and the rate constants in Table 1. The starting conditions for regeneration were (a) 8.0 μM protein and 40 mM DTT^{ox}; (b) 15 μM protein and 150 mM DTT^{ox}; (c) 32 μM protein and 150mM DTT^{ox}; (d) 15 μM protein and 200 mM DTT^{ox}.

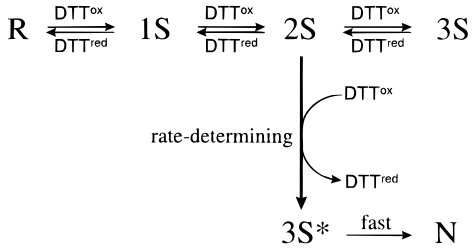

FIGURE 4: Best-fit regeneration pathway for des-[40−95]A. The rate constants are given in Table 1. R, 1S, 2S, 3S, and N represent reduced protein, one-disulfides, two-disulfides, three-disulfides, and native protein, respectively. The bimolecular rate constant for the rate-limiting step, 2S → 3S*, is equal to $(5.1 \pm 0.1) \times 10^{-3}$ min^{-1} M^{-1}. The identity of 3S* is discussed in the text.

phenomenon), rather than the occurrence of new intermediates. This suggests that the interconversion between different species within each disulfide grouping (disulfide reshuffling) is much more rapid than the formation of an additional disulfide bond. Therefore, each group of disulfide intermediates can be treated as a single kinetic species.

Figure 3 shows plots of the concentration changes as a function of regeneration time for the different disulfide-bonded species under four different regeneration conditions. The experimental data, indicated by various symbols, represent different sets of disulfide groupings as specified in the figure legend. The solid curves represent the results from fitting the experimental data with a kinetic model, which will be presented in detail in the next subsection. Several regeneration experiments were carried out under various redox conditions by changing the initial concentrations of reduced protein and DTT^{ox}. It is clear that the concentrations of the groups of disulfide-bonded species follow similar steady-state kinetics under all the regeneration conditions. However, the time required for the attainment of the steady-state condition depends on the initial redox potential. In addition, the relative concentration of each disulfide grouping in the steady-state also depends on the initial redox condition.

Fitting of Kinetic Data. To extract information about the folding pathway, the experimental data were fit to various models considering all possible single folding pathways. This approach makes no assumptions concerning the intermediates that are involved in the rate-determining step. Rather, it considers that all species present in the steady state may undergo a rate-determining transition that will convert it into an intermediate that will fold rapidly to the native protein. This approach has been used successfully in fitting the data from kinetic studies for both wild-type RNase A (containing four disulfide bonds) (*11*) and recombinant hirudin variant 1 (rHV1) (containing three disulfide bonds) (*34*). The experimental data for this three-disulfide mutant, des-[40−95]A, are fit similarly in the present work.

There are three different types of reactions that can be involved in a rate-determining step: oxidation, reduction, and rearrangement. As for the three-disulfide hirudin, there are 10 possible rate-determining steps (see Figure 3 of reference *34*) in the regeneration of des-[40−95]A. Combined with the steady-state condition for the folding intermediates, the experimental data under all redox conditions were fit to each of the single-pathway models. The best fit was obtained for a model which assumes a single major regeneration pathway in which the rate-determining step involves the formation of a three-disulfide species (3S*) from one or more two-disulfide intermediates (2S). The kinetic pathway corresponding to this model for the regeneration of des-[40−95]A is depicted in Figure 4. The goodness of fit is shown in Figure 3 using solid curves (computed with the rate constants of Table 1) overlaid on the symbols representing the experimental data. It is clear that this model fits every regeneration condition very well, suggesting the suitability of this model as a representation of the data. It must be pointed out that 3S* is a species formed after the rate-determining step which is kinetically indistinguishable from the native protein and proceeds rapidly to form the native protein (N). It presumably has the correct disulfide bonds but may have a conformation that is different from that of N, or, more likely, is N itself. However, there is no experimental evidence to support the existence of a 3S* species that is different from N. It is included in the model to allow for the possibility of rapid conformational rearrangements after the rate-determining step.

By fitting the experimental data with this kinetic model, several kinetic parameters can be derived. These include the rate constants for formation and reduction of disulfide bonds at different stages of disulfide bond formation, the equilibrium constants between different disulfide groupings under the steady-state conditions, and the rate constant for the rate-determining step. The results are summarized in Table 1. The forward rate constants are denoted as k_f (for reactions R → 1S, 1S → 2S, 2S → 3S), the back-reaction rate constants are denoted as k_r (for reactions 1S → R, 2S → 1S, and 3S → 2S), and the equilibrium constants are denoted as K.

Since each disulfide grouping was treated as a single species in our kinetic model, the resulting rate and equilibrium constants are a weighted sum over all the single-

Table 1: Rate and Equilibrium Constants[a] for the Regeneration of Des-[40−95]A at 25 °C and pH 8.0

reaction	$(k^{obs})_f$ $(\times 10^2)$ $(min^{-1}\ M^{-1})$	$(k^{ave})_f$ $(\times 10^2)$ $(min^{-1}\ M^{-1})$	$(k^{obs})_r$ $(\times 10^{-2})$ $(min^{-1}\ M^{-1})$	$(k^{ave})_r$ $(\times 10^{-2})$ $(min^{-1}\ M^{-1})$	K^{obs} $(\times 10^4)$	K^{ave} $(\times 10^4)$
R ↔ 1S	75.8 ± 0.6	5.0 (15)	3.0 ± 0.08	3.0 (1)	25.3	1.7
1S ↔ 2S	16.4 ± 0.2	2.7 (6)	5.7 ± 0.04	2.8 (2)	2.9	0.96
2S ↔ 3S	2.0 ± 0.2	2.0 (1)	11.5 ± 1.1	3.8 (3)	0.17	0.52
2S → 3S*		0.51				

[a] These rate and equilibrium constants were determined from data for the whole time course of the reaction under eight different experimental redox conditions. $(k^{obs})_f$ and $(k^{obs})_r$ are the observed forward and reverse rate constants for the formation or reduction of a disulfide bond using DTT^{ox} and DTT^{red}, respectively. $(k^{ave})_f$ and $(k^{ave})_r$ are the average forward and reverse rate constants, respectively, obtained by correcting the observed rate constants with the corresponding statistical factors indicated by the numbers in parentheses. K^{obs} is the observed equilibrium constant between different disulfide species under steady-state conditions. K^{ave} is computed by taking the ratios of $(k^{ave})_f$ over $(k^{ave})_r$. 2S → 3S* is the rate-determining step for the regeneration of des-[40−95]A. Errors are calculated at the 95% confidence limit.

disulfide intermediates in that grouping. This treatment is valid because the distribution for each group of disulfide-bonded intermediates is invariant to the regeneration time and the initial redox conditions. It is not possible to obtain information about specific disulfide-bonded species because there are many chemically distinct disulfide-bonded species within each disulfide grouping. However, we can calculate an average rate and equilibrium constant for a disulfide-bonded species assuming that every disulfide-bonded species within a disulfide grouping is kinetically homogeneous. Although these average rate and equilibrium constants might differ greatly from those for any single species, this is the only information that can be obtained, considering the large number of intermediates in this system and the method used for the kinetic treatment. Nonetheless, such average rate and equilibrium constants yield useful information concerning the folding pathways and conformations of disulfide-bonded intermediates. The average rate and equilibrium constants were obtained by applying a statistical factor to the overall observed data for each disulfide grouping, and these average values are also listed in Table 1. The statistical factors were calculated by considering all the possible number of disulfide intermediates involved in the regeneration process. For example, there are 15 possible one-disulfide intermediates that could form from 1 fully reduced species through disulfide-bond formation; therefore, the average formation rate constant for the first disulfide bond is equal to the observed value divided by 15. The statistical factors applied in the calculation are also listed in Table 1.

It is interesting to note from Table 1 that the rate constants for formation of a disulfide bond are different at different regeneration stages. The average rate constant for formation of a disulfide bond becomes smaller as the number of disulfide bonds in the disulfide-bonded species increases. However, the average reduction rate constants do not vary very much. The second-order rate constant for the rate-determining step (2S → 3S*) is 5.1×10^{-3} min^{-1} M^{-1}, i.e., about a factor of 10 smaller than that for the formation of the first disulfide bonds (R → 1S, 5.0×10^{-2} min^{-1} M^{-1}) and a factor of 4 smaller than that for the formation of the third disulfide bond (2S → 3S, 2.0×10^{-2} min^{-1} M^{-1}). The average equilibrium constants follow a similar trend as the average forward rate constants which decrease as the number of disulfide bonds increases, suggesting that the difference in stabilization energy between 1S and R is larger than that between 2S and 1S, which again is larger than that between 3S and 2S.

Comparison with the Folding Kinetics of Wild-Type RNase A. A comparison of the folding kinetics for both the mutant and wild-type RNase A is necessary in order to obtain information about the folding of this three-disulfide mutant and the conformations of its disulfide-bonded folding intermediates. The kinetic parameters are listed in Table 2. The parameters for wild-type RNase A were obtained from the paper by Rothwarf et al. (*15*). Since wild-type ribonuclease A contains one more disulfide bond than the three-disulfide mutant, and the kinetic model contains two more rate constants, a complete comparison is not possible. Instead, only the relevant parameters are listed in Table 2. From Table 2, it is interesting to note that the average rate constants for formation of the first disulfide bond are very similar for both proteins (5.0×10^{-2} min^{-1} M^{-1} vs 5.2×10^{-2} min^{-1} M^{-1}, respectively), suggesting that the early folding processes might be similar in these two proteins, driven by similar types of interatomic interactions. However, the formation rate constants in the mutant follow a different trend from those in wild-type RNase A; e.g., in wild-type RNase A, they do not vary much at different stages of folding, while the corresponding rate constants become progressively smaller in des-[40−95]A. On the other hand, the average reduction rate constants do not differ much at different stages of reduction for both the mutant and wild-type RNase A, although the rate constants are generally about a factor of 2 smaller in des-[40−95]A.

Table 2: Comparison of Rate and Equilibrium Constants[a] between Des-[40−95]A and Wild-Type RNase A

	$(k^{ave})_f$ ($\times 10^2$) (min^{-1} M^{-1})		$(k^{ave})_r$ ($\times 10^{-2}$) (min^{-1} M^{-1})		K^{ave} ($\times 10^4$)	
reaction	mutant	WT	mutant	WT	mutant	WT
R ↔ 1S	5.0	5.2	3.0	5.2	1.7	1.0
1S ↔ 2S	2.7	5.0	2.8	5.6	0.96	0.89
2S ↔ 3S	2.0	6.2	3.8	6.3	0.52	0.98

[a] $(k^{ave})_f$ and $(k^{ave})_r$ are the average rate constants for formation or reduction of a disulfide bond. K^{ave} are the average equilibrium constants between different groups of disulfide intermediates under steady-state conditions. Data for mutant des-[40−95]A are from the present work as listed in Table 1. Data for wild-type (WT) RNase A were adopted from the work of Rothwarf et al. (ref. *15*). The rate constant for the rate-determining step (2S → 3S*) in des-[40−95]A is 5.1×10^{-3} min^{-1} M^{-1}, while that for the rate-limiting step (3S → 3S*) in wild-type RNase A is 1.4×10^{-2} min^{-1}.

Comparison of the equilibrium constants shows that they decrease by more than a factor of 3 (from 1.7 to 0.52 in Table 2) as the number of disulfide bonds increases in the mutant, while little variation is observed for the equilibrium constants in wild-type RNase A. This is the result of different trends in the average disulfide bond formation and reduction rate constants for this mutant and wild-type RNase A. These data suggest that the stability difference between 1S and R in this mutant is larger than that in wild-type RNase A; the stability difference between 2S and 1S in the mutant is similar to that in wild-type RNase A; and the stability difference between 3S and 2S is smaller in the mutant than that in wild-type RNase A.

It is also notable that oxidative regeneration of des-[40−95]A and RNase A undergoes different rate-determining steps: e.g., 2S → 3S* for des-[40−95]A and 3S → 3S* for wild-type RNase A, respectively, suggesting that at least two pathways are possible for the formation of the three-disulfide intermediate des-[40−95] during the regeneration of wild-type RNase A. The rate constant for formation of des-[40−95]A through 2S → 3S* is 0.51×10^{-2} min^{-1} M^{-1}, while that for des-[40−95] through 3S → 3S* is 1.4×10^{-2} min^{-1} (*15*). Since the maximal concentration of DTT^{ox} used was 200 mM, a rough estimation would suggest that the pathway of 2S → 3S* (approximately $0.2 \times 0.51 \times 10^{-2} = 0.1 \times 10^{-2}$ min^{-1}) is much slower than that of 3S → 3S*. A detailed account of how these two pathways compete in the regeneration of RNase A will be given below under Discussion.

DISCUSSION

The kinetic study of the oxidative regeneration pathway of des-[40−95]A suggests that the majority of the protein

refolds through a pathway with the rate-determining step 2S → 3S*. Since 3S* presumably contains three native disulfide bonds, but with a possibly different conformation from the native mutant, there is only a limited number of 2S species that can serve as the direct precursor for this rate-determining step. In fact, only three two-disulfide intermediates can be involved in the rate-determining step leading directly to the formation of 3S*; each of them contains two of the three native disulfide bonds. Other 2S species have to rearrange to form one of these three direct precursors to form 3S*. It is not clear at the present time whether all three two-disulfide intermediates are involved as direct precursors in the rate-determining step. It must be pointed out that the regeneration rate is much slower for des-[40−95]A than that for wild-type RNase A under the same redox conditions (footnote *a*, Table 2), possibly because des-[40−95]A is less stable than wild-type RNase A (*35*). Higher concentrations of oxidizing reagent or lower concentrations of protein were required to achieve a practical regeneration rate for des-[40−95]A. Therefore, the redox potentials for the regeneration of the mutant cannot be varied over as wide a range as that for RNase A, simply because the available DTT^{ox} and protein concentrations are more limited for des-[40−95]A than those for wild-type RNase A. It must also be pointed out that the rate-determining step can change under different redox conditions. Under very high oxidizing conditions (perhaps 100 or 1000 times higher, which is not possible in this case because of the limited solubility of DTT^{ox}), the formation of 3S* from 2S could become much faster with little dependence on the oxidant concentration. The rate-determining step could then become the rearrangement of the 2S species to form certain 2S* which could lead to a rapid formation of the native protein through oxidation.

The primary interest in studying the regeneration of des-[40−95]A is to gain further understanding about the folding pathways of wild-type RNase A, since the corresponding three-disulfide intermediate (des-[40−95]) was found to form in a rate-determining step in the regeneration of wild-type RNase A. In addition, the kinetic study of the regeneration of RNase A showed that over 80% of the protein regenerates through the formation of this three-disulfide intermediate, suggesting its importance in the folding of RNase A. However, there is a potential limitation in using a mutant for the regeneration study to mimic the true three-disulfide intermediates. Although the substitutions of Cys40 and Cys95 eliminated the formation of disulfide bond [40−95], they also eliminate those disulfide exchange reactions (e.g., disulfide bond oxidation, disulfide bond reduction, and disulfide rearrangement) involving these two cysteines during the regeneration process. Therefore, the disulfide rearrangement pathway for the formation of des-[40−95] in the regeneration of RNase A is no longer possible for the regeneration of the mutant des-[40−95]A. The regeneration of des-[40−95]A has to follow alternative pathways. The experiments with this mutant provide an opportunity to study those unpreferred pathways in the regeneration of RNase A in detail. In addition, the rate constants obtained from the kinetic study can provide information about the conformations of disulfide intermediates for this mutant protein as well as for the wild-type RNase A.

Conformations of Disulfide-Bonded Intermediates at Various Stages of Regeneration. Comparison of the rate constants for formation and reduction of disulfide bonds at various stages of regeneration can provide important information about the average conformations assumed by the different groupings of disulfide-bonded intermediates in the mutant protein. A smaller rate constant for formation of a disulfide bond indicates that the conformations of the disulfide intermediates are more restricted, hindering the formation of the additional disulfide bond. From Table 1, it is seen that the average formation rate constant becomes smaller as the number of disulfide bonds in the intermediates increases. Therefore, the data suggest that the one-, two-, and three- disulfide intermediates have progressively more structured conformations. The average formation rate constant for R → 1S is almost twice that for 1S → 2S, suggesting that 1S is significantly more structured than R. The structured conformations in 1S slow down the formation of the second disulfide bond by restricting the mobility of other cysteine residues. In an analogous way, 2S is slightly more structured in conformation than 1S, as the formation rate constant for 2S → 3S is only slightly smaller than that for 1S → 2S.

The reduction rate constants of disulfide bonds are also affected by the conformations of disulfide-bonded intermediates; however, the mobility of free thiols is no longer the determining factor for reduction rates as it is for oxidation rates. This is probably the reason why different trends were observed for oxidation and reduction rate constants. The reduction rate constants depend on the accessibility of the disulfide bonds in proteins to small thiol reagents. If a protein has a compact structure, some disulfide bonds would be buried inside, and reduction of these disulfide bonds would become difficult. On the other hand, if a protein structure is dynamic and not well packed, small thiol molecules could penetrate into the inside of the protein frequently, which would greatly enhance the reduction rate constant for those buried disulfide bonds. From Table 1, it is found that the reduction rate constants at various stages of regeneration are very similar, suggesting that the conformations assumed by all groupings of disulfide-bonded intermediates are dynamic, although localized structures may exist to various extent in different folding intermediates. It is not surprising to find that the structures of different groupings of disulfide-bonded intermediates are dynamic, since an NMR study also revealed a dynamic structure for the mutant des-[40−95]A from H/D exchange experiments (*24*), even though a significant amount of native-like structure exists in this mutant.

Implications for the Folding of Wild-Type RNase A. Comparison of the kinetic constants derived from the regeneration studies for both the mutant and wild-type RNase A reveals useful information about the folding of wild-type RNase A. It is interesting to note that the average formation rate constants of 1S from R are very similar for the mutant and wild-type RNase A (see Table 2), indicating that both proteins might fold similarly at early times. The involvement of Cys40 or Cys95 in the formation of disulfide pairing is not significant in the early folding stage. This probably results from the predominance of a 1S species containing the disulfide bond between Cys65 and Cys72 at the one-disulfide stage. Characterization of the one-disulfide intermediates formed during the regeneration of wild-type RNase A showed that this 1S species comprises up to 40% of the

whole mixture, while the average population of the 1S species containing Cys40 or Cys95 is only 2% (*25*). Preliminary results from a study of the distribution of the one-disulfide mixture formed during regeneration of des-[40−95]A also revealed that the 1S species containing Cys65 and Cys72 is the dominant species (X. Xu and H. A. Scheraga, unpublished results). Regeneration studies of another three-disulfide mutant des-[65−72]A lacking Cys65 and Cys72 (which, therefore, cannot form the otherwise favored 65−72 disulfide bond) showed that the average formation rate constant for R → 1S is a factor of 2 *smaller* than that for des[40−95]A (*26*). These results indicate that formation of the disulfide bond between Cys65 and Cys72 is favored both kinetically and thermodynamically over other disulfide pairings. Therefore, it is conceivable that, in the early folding stage, the absence of a couple of cysteines other than Cys65 and Cys72 will not lead to a marked difference in the average rate constant for formation of the one-disulfide species.

The average formation rate constants for 1S → 2S and 2S → 3S are a factor of 2−3 smaller in the mutant than in wild-type RNase A. There are several factors that could contribute to the observed rate constants for disulfide exchange reactions. These include electrostatic and other sequence-specific local interactions, entropic contributions, and steric factors. The details about how these factors affect the observed rate constants have been discussed elsewhere (*34*). Comparing the sequences of des-[40−95]A and wild-type RNase A, only two residues were substituted. Therefore, most of those factors will have similar effects on both proteins. However, it seems that two factors can contribute to the observed variations in formation rate constants for the mutant protein. One is the enthalpic contribution accompanying structure formation due to the favorable formation of disulfide bond 65−72. A preliminary study of the distribution of disulfide intermediates formed in the regeneration of des-[40−95]A suggested that about 50% of the one-disulfide intermediates contain the disulfide bond 65−72. The percentage of species containing this 65−72 disulfide bond is higher for the two-disulfide intermediates than for the one-disulfide intermediates, and this percentage is even higher for the three-disulfide intermediates (X. Xu and H. A. Scheraga, unpublished results). It seems that the formation of the 65−72 disulfide bond leads to progressively more structured conformations in disulfide intermediates at the 1S, 2S, and 3S stages, resulting in slower disulfide bond formation rates.

A second factor could arise from entropic contributions, because removal of Cys40 and Cys95 eliminates formation of some shorter disulfide loops. In the sequence of RNase A, residue Cys40 lies between Cys26 and Cys58, and Cys95 lies between Cys84 and Cys110. Therefore, the average length of the disulfide loops is greater in the mutant des-[40−95]A than in wild-type RNase A. During the regeneration of a protein through disulfide bond formation, shorter disulfide loops would form preferentially because a smaller entropy loss is involved. Based on this consideration, it is expected that the average formation rate of a disulfide bond in the mutant protein would be slower than that in wild-type RNase A. However, since the two shortest disulfide loops (58−65 and 65−72) remain intact in the mutant protein, such an entropic effect is small. Therefore, the average formation rate for one-disulfide intermediates does not differ much between the mutant and wild-type RNase A. The effect of entropy on the formation rates of the second and third disulfide bonds becomes more complicated because of the presence of overlapping disulfide loops. The presence of these overlapping disulfide loops can reduce the entropic effects. As a consequence, the average rates for formation of the second and third disulfide bonds in the mutant remain similar to that for the first disulfide bond in the regeneration of wild-type RNase A (*15*). It seems that the effect of conformational restriction on the average formation rate constants introduced by preferential formation of disulfide bond 65−72 dominates over the entropic effects, resulting in decreased average formation rate constants for 2S and 3S in the mutant protein des-[40−95]A.

The average reverse rate constants for disulfide reduction in des-[40−95]A were found to be about a factor of 2 smaller than those in wild-type RNase A at all regeneration stages. There are 15 possible different one-disulfide bonds in each disulfide grouping for des-[40−95]A and 28 possible different one-disulfide bonds for wild-type RNase A. It is conceivable that the reduction of each grouping of disulfide intermediates occurs by first reducing some disulfide bonds that are easier to break followed by rapid reshuffling of other disulfide bonds to these disulfide bonds. It is known that the rate for disulfide reshuffling is much faster than the rate of reduction. Therefore, the reduction rate for each disulfide grouping is determined by the reduction rates for those rapidly reducing disulfide bonds. The slower reduction rate constants in mutant des-[40−95]A could result from the presence of faster reducing disulfide bonds in wild-type RNase A which are absent in the mutant des-[40−95]A. Apparently those disulfide bonds would have to involve either Cys40 or Cys95 in the wild-type protein. Examination of the sequence of wild-type RNase A indicates that, of all eight cysteines in the amino acid sequence, Cys40 is the only residue which has two neighboring positively charged residues (R39 and K41). The positive charges around cysteine can render that disulfide bond more susceptible to a disulfide bond exchange reaction with a reactive S^- species. It is likely that those disulfide bonds containing Cys40 have faster reduction rates than other disulfide bonds, resulting in a faster reduction rate for each disulfide grouping in wild-type RNase A. This idea is supported by reduction experiments in which the 40−95 disulfide bond has a faster reduction rate than that for 65−72 at 25 °C (*32*). Further supporting evidence also comes from the kinetic measurements of the regeneration of the other mutant, des-[65−72]A, containing cysteines 40 and 95 but missing cysteines 65 and 72 (*26*); it was found that the average reduction rate constant for each disulfide grouping of this mutant (des-[65−72]A) is very similar to that for wild-type RNase A.

Comparison of the rate-determining steps in the mutant and wild-type RNase A provides additional information about folding processes that occur in wild-type RNase A. In the mutant protein, both Cys40 and Cys95 were replaced by alanines. Therefore, those kinetic steps, such as disulfide bond formation, reduction, and reshuffling, involving Cys40 or Cys95 could not occur in the regeneration of the mutant protein. It is apparent that these kinetic steps are important in the refolding of wild-type protein because two different folding pathways were observed. It is clear that the rate-determining step 3S → 3S* for wild-type RNase A cannot

serve as the rate-determining step in the mutant protein because no free thiols are present in 3S to facilitate this type of rearrangement. However, it is possible that the rate-determining step for the mutant protein 2S → 3S* could possibly serve as one of the rate-determining steps in the refolding of wild-type RNase A.

The likelihood of occurrence of this pathway in the regeneration of wild-type RNase A can be evaluated by assuming that a competitive pathway with the rate-determining step 2S → des-[40−95] exists in the regeneration of wild-type RNase A in addition to the major pathway containing the rate-determining step 3S → des-[40−95]. The competition between these two pathways can be expressed as

$$\frac{R_1}{R_2} = \frac{k_1[2S][DTT^{ox}]}{k_2[3S]} = \frac{k_1[DTT^{red}]}{k_2 K_3} \qquad (2)$$

where R_1 and R_2 represent reaction rates for reactions 2S → des-[40−95] and 3S → des-[40−95], respectively, k_1 and k_2 are the rate constants for both reactions, and K_3 is the equilibrium constant between 2S and 3S for wild-type RNase A. It must be noted that k_1 is different from that for the rate-determining step in the mutant des-[40−95]A, because different two-disulfide intermediates are present in the mutant and wild-type RNase A. There are 45 possible two-disulfide intermediates involved in the mutant and 210 possible two-disulfide intermediates involved in wild-type RNase A. Since only a small fraction of the two-disulfide intermediates in wild-type RNase A can proceed through oxidation to form des-[40−95] with the rate constant of 0.51×10^{-2} min^{-1} M^{-1} (the rate-determining step for the mutant protein), the number k_1 can be estimated roughly as $0.51 \times 10^{-2} \times 45/210 = 0.11 \times 10^{-2}$ min^{-1} M^{-1}; k_2 is 1.4×10^{-2} min^{-1}, the rate constant for formation of des-[40−95] in wild-type RNase A (*15*), and K_3 is 0.98×10^{-4} (*15*). In the regeneration of wild-type RNase A, the typical concentrations of $[DTT^{red}]$ at steady-state are between 10 and 70 μM (*10*, *11*). Therefore, the ratio R_1/R_2 is in the range of 0.8−5.6%. It is apparent that the regeneration pathway through 2S → des-[40−95] is only a minor pathway for the refolding of wild-type RNase A, if it exists. This pathway will become dominant only when the major pathway 3S → des-[40−95] is blocked as in the case of the mutant studied in this investigation.

Comparison with Folding Studies of Other Three-Disulfide-Containing Proteins. The folding of several proteins containing three disulfide bonds has been studied using the disulfide bond formation method. Bovine pancreatic trypsin inhibitor (BPTI) is one of the most extensively studied three-disulfide proteins. Its disulfide folding pathways have been well characterized, although controversies still exist over the role of non-native disulfide species (*5*, *7*−*9*, *36*−*38*). Thannhauser et al. (*34*) have studied the oxidative regeneration of a three-disulfide-bonded hirudin, recombinant hirudin variant 1 (rHV1). Recently, Iwaoka et al. (*26*) have studied the regeneration pathway of another three-disulfide mutant, des-[65−72]A (replacing Cys65 and Cys72 with alanines in wild-type RNase A), using a technique similar to the one described in this paper.

Comparison of the oxidative refolding pathways in these proteins indicates that rHV1, des-[65−72]A, and des-[40−95]A refold through similar folding pathways with a common rate-determining step of 2S → 3S*. However, the average rate constants for disulfide bond formation and reduction at different folding stages as well as that for the rate-determining step differ among these three proteins. BPTI folds very differently from these proteins. One of the main differences is in the appearance of disulfide intermediates. In BPTI, only three stable one-disulfide intermediates and two stable two-disulfide intermediates were observed in the folding of BPTI (*8*). In rHV1, des-[65−72]A, and des-[40−95]A, the refolding is accompanied by formation of many disulfide-bonded intermediates (containing both native and non-native disulfide bonds) which undergo rapid disulfide reshuffling within each grouping containing the same number of disulfide bonds. The formation of a large number of disulfide intermediates was also observed for several other proteins studied using the disulfide-mediated technique (*39*−*41*). It seems that formation of a large number of disulfide-bonded intermediates during oxidative refolding may be a common feature for most proteins. BPTI probably represents a special case.

The unusual folding property of BPTI may result from its exceptional stability. It is well-known that BPTI is unusually resistant to denaturation by temperature, urea, or guanidine hydrochloride (*42*, *43*). It is also apparent that those disulfide intermediates observed in the folding of BPTI are stable because of their native-like structures. It seems that the stable native-like conformation in BPTI makes a few disulfide intermediates much more stable than other disulfide intermediates with different disulfide pairings. Since disulfide reshuffling happens very fast, those unstable intermediates reshuffle to form the more stable species, and, therefore, only those stable species are observed predominantly in the folding of BPTI. This idea is supported by the observation of several other one-disulfide species (in addition to the three stable species) at early refolding times in the study of BPTI (*38*). On the other hand, the two mutants of RNase A (des-[40−95]A and des-[65−72]A) have much lower thermal stability with $T_m = 33.7$ °C for des-[40−95]A and $T_m = 38.5$ °C for des-[65−72]A at pH 4.6 (*23*, *24*). Therefore, for these proteins with less stability, the native conformation does not stabilize some disulfide intermediates significantly more than others. As a consequence, a large number of one-, two-, and three- disulfide intermediates with comparable conformational stability were observed during oxidative regeneration. However, a small difference in conformational stability might exist among the different disulfide intermediates because of the presence of local structures which could result in nonrandom distributions for different groupings of disulfide intermediates. This behavior was clearly observed for the distribution of one-disulfide intermediates formed during the regeneration of wild-type RNase A (*25*).

It is apparent that, in the oxidative refolding of a protein, the appearance of disulfide intermediates is intrinsically related to the conformation of the disulfide-bonded intermediates as well as to the intrinsic stability of the native protein. The folding of most proteins probably occurs through the formation of a variety of disulfide-bonded intermediates that reflect their conformational stability as well as the structural transitions in the folding processes. The folding of BPTI is probably one of the extreme cases,

although it has served as one example in the study of disulfide folding pathways. It must be mentioned that the approaches developed in our laboratory to study protein folding through disulfide bond formation provide a unique way to separate different disulfide groupings. In addition, the redox potential in our experiments is well controlled, providing the possibility of fitting the experimental data with kinetic models. Therefore, this method can be applied directly to the study of disulfide folding pathways for disulfide-containing proteins in general.

ACKNOWLEDGMENT

We thank D. M. Rothwarf for helpful discussions and suggestions and Y.-J. Li for assistance with some of the experiments.

REFERENCES

1. Matthews, C. R. (1993) *Annu. Rev. Biochem. 62*, 653.
2. Roder, H. (1995) *Nat. Strut. Biol. 2*, 817.
3. Baldwin, R. L. (1996) *Folding Des. 1*, R1.
4. Fersht, A. R. (1997) *Curr. Opin. Struct. Biol. 7*, 3.
5. Creighton, T. E. (1977) *J. Mol. Biol. 113*, 329.
6. Scheraga, H. A., Konishi, Y., and Ooi, T. (1984) *Adv. Biophys. 18*, 21.
7. Creighton, T. E., and Goldenberg, D. P. (1984) *J. Mol. Biol. 179*, 497.
8. Weissman, J. S., and Kim, P. S. (1991) *Science 253*, 1386.
9. Weissman, J. S., and Kim, P. S. (1992) *Proc. Natl. Acad. Sci. U.S.A. 89*, 9900.
10. Rothwarf, D. M., and Scheraga, H. A. (1993) *Biochemistry 32*, 2671.
11. Rothwarf, D. M., and Scheraga, H. A. (1993) *Biochemistry 32*, 2680.
12. Rothwarf, D. M., and Scheraga, H. A. (1993) *Biochemistry 32*, 2690.
13. Rothwarf, D. M., and Scheraga, H. A. (1993) *Biochemistry 32*, 2698.
14. Rothwarf, D. M., Li, Y.-J., and Scheraga, H. A. (1998) *Biochemistry 37*, 3760.
15. Rothwarf, D. M., Li, Y.-J., and Scheraga, H. A. (1998) *Biochemistry 37*, 3767.
16. Hantgan, R. R., Hammes, G. G., and Scheraga, H. A. (1974) *Biochemistry 13*, 3421.
17. Creighton, T. E. (1979) *J. Mol. Biol. 129*, 411.
18. Anfinsen, C. B., and Scheraga, H. A. (1975) *Adv. Protein Chem. 29*, 205.
19. Konishi, Y., and Scheraga, H. A. (1980) *Biochemistry 19*, 1308.
20. Konishi, Y., and Scheraga, H. A. (1980) *Biochemistry 19*, 1316.
21. Rothwarf, D. M., and Scheraga, H. A. (1991) *J. Am. Chem. Soc. 113*, 6293.
22. Talluri, S., Rothwarf, D. M., and Scheraga, H. A. (1994) *Biochemistry 33*, 10437.
23. Shimotakahara, S., Rios, C. B., Laity, J. H., Zimmerman, D. E., Scheraga, H. A., and Montelione, G. T. (1997) *Biochemistry 36*, 6915.
24. Laity, J. H., Lester, C. C., Shimotakahara, S., Zimmerman, D. E., Montelione, G. T., and Scheraga, H. A. (1997) *Biochemistry 36*, 12683.
25. Xu, X., Rothwarf, D. M., and Scheraga, H. A. (1996) *Biochemistry 35*, 6406.
26. Iwaoka, M., Juminaga, D., and Scheraga, H. A. (1998) *Biochemistry 37*, 4490.
27. delCardayré, S. B., Ribo, M., Yokel, E. M., Quirk, D. J., Rutter, W. J., and Raines, R. T. (1995) *Protein Eng. 8*, 261.
28. Bruice, T. W., and Kenyon, G. L. (1982) *J. Protein Chem. 1*, 47.
29. Ellman, G. L. (1959) *Arch. Biochem. Biophys. 82*, 70.
30. Thannhauser, T. W., Konishi, Y., and Scheraga, H. A. (1984) *Anal. Biochem. 138*, 181.
31. Rothwarf, D. M., and Scheraga, H. A. (1992) *Proc. Natl. Acad. Sci. U.S.A. 89*, 7944.
32. Li, Y.-J., Rothwarf, D. M., and Scheraga, H. A. (1995) *Nat. Struct. Biol. 2*, 489.
33. Konishi, Y., Ooi, T., and Scheraga, H. A. (1982) *Biochemistry 21*, 4734.
34. Thannhauser, T. W., Rothwarf, D. M., and Scheraga, H. A. (1997) *Biochemistry 36*, 2154.
35. Laity, J. H., Shimotakahara, S., and Scheraga, H. A. (1993) *Proc. Natl. Acad. Sci. U.S.A. 90*, 615.
36. Creighton, T. E. (1992) in *Protein Folding* (Creighton T. E., Ed.) pp 301−351, W. H. Freeman, New York.
37. Darby, N. J., Morin, P. E., Talbo, G., and Creighton, T. E. (1995) *J. Mol. Biol. 249*, 463.
38. Dadlez, M., and Kim, P. S. (1995) *Nat. Struct. Biol. 2*, 674.
39. Chatrenet, B., and Chang, J.-Y. (1993) *J. Biol. Chem. 268*, 20988.
40. Chang, J.-Y., Schindler, P., and Chatrenet, B. (1995) *J. Biol. Chem. 270*, 11992.
41. Chang, J.-Y. (1996) *Biochemistry 35*, 11702.
42. Moses, E., and Hinz, H. J. (1983) *J. Mol. Biol. 170*, 765.
43. Makhatadze, G. I., Kim, K. S., Woodward, C., and Privalov, P. L. (1993) *Protein Sci. 2*, 2028.

BI980086X